

Geophysical Research Letters

RESEARCH LETTER

10.1029/2019GL085340

Key Points:

- PMM and WNP TC variability show a strong relationship on quasi-decadal timescales but less so on interannual timescales
- PMM and central Pacific ENSO-like SST variability are indistinguishable on quasi-decadal timescales
- Equatorial Pacific SST variability impacts WNP TCs on both interannual and decadal timescales

Supporting Information:

- Supporting Information S1

Correspondence to:

W. Zhang,
zhangwj@nuist.edu.cn

Citation:

Liu, C., Zhang, W., Stuecker, M. F., & Jin, F.-F. (2019). Pacific Meridional Mode-Western North Pacific Tropical Cyclone Linkage Explained by Tropical Pacific Quasi-Decadal Variability. *Geophysical Research Letters*, 46, 13,346–13,354. <https://doi.org/10.1029/2019GL085340>

Received 9 SEP 2019

Accepted 24 OCT 2019

Accepted article online 3 NOV 2019

Published online 22 NOV 2019

Pacific Meridional Mode-Western North Pacific Tropical Cyclone Linkage Explained by Tropical Pacific Quasi-Decadal Variability

Chao Liu¹, Wenjun Zhang¹ , Malte F. Stuecker^{2,3} , and Fei-Fei Jin⁴ 

¹CIC-FEMD/ILCEC, Key Laboratory of Meteorological Disaster of Ministry of Education (KLME), Nanjing University of Information Science and Technology, Nanjing, China, ²Center for Climate Physics, Institute for Basic Science (IBS), Republic of Korea, ³Busan, Republic of Korea, ⁴Department of Atmospheric Sciences, SOEST, University of Hawai'i at Mānoa, Honolulu, HI, USA

Abstract Previous studies argued that the Pacific Meridional Mode (PMM) impacts tropical cyclone (TC) genesis variability over the southeastern part of the western North Pacific (SE-WNP). Here, we find that the statistical relationship between PMM and SE-WNP TC genesis frequency is dominated by their co-variability on decadal timescales. The decadal component of the PMM exhibits very similar temporal and spatial features to quasi-decadal tropical Pacific sea surface temperature (SST) variability. The latter can affect SE-WNP TC activity via changes in both zonal vertical wind shear and low-level vorticity. In contrast, the interannual component of the PMM exhibits no statistically significant correlation with SE-WNP TC genesis. Furthermore, observations show that both interannual and decadal variability of SE-WNP TC activity are well correlated with the commonly used Niño3.4 El Niño-Southern Oscillation index. Thus, equatorial Pacific SST variability is the dominant source of SE-WNP TC activity predictability on different timescales.

1. Introduction

The tropical cyclone (TC) genesis frequency over the western North Pacific (WNP; 0°–40°N, 100°E–180°) exhibits pronounced interannual variability, which has been widely investigated in the past few decades (e.g., Wang and Chan 2002; Camargo et al., 2007; Zhang et al., 2017b). Specifically, the El Niño-Southern Oscillation (ENSO)—the predominant source of global interannual climate variability (e.g., McPhaden et al., 2006; Timmermann et al., 2018; Wallace et al., 1998)—strongly modulates year-to-year WNP TC activity (e.g., Kim et al., 2011; Wang & Chan, 2002). Importantly, it was found that ENSO primarily influences the spatial distribution rather than the total number of WNP TC genesis during its developing summer phase (e.g., Wang & Chan, 2002). In contrast, during the decaying phase of El Niño, WNP TC activity is usually suppressed, as the WNP is characterized by large-scale low-level anomalous anticyclonic circulation (Du et al., 2011; Wang & Chan, 2002). During the recent two decades, the statistical ENSO-TC relationship is complicated by the more frequent occurrence of central Pacific (CP) El Niño events (e.g., Ashok et al., 2007; Kao & Yu, 2009; Kug et al., 2009). The anomalous air-sea interaction center during CP El Niño events is shifted toward the dateline compared to traditional El Niño events that exhibit maximum sea surface temperature (SST) anomalies in the eastern equatorial Pacific. In contrast to traditional El Niño events, CP El Niño is usually accompanied by a basin-wide enhancement of TC activity during its developing phase in boreal summer and a minor suppression during its decaying phase the following summer (e.g., Chen & Tam, 2010; Kim et al., 2011; Wang et al., 2013; Wang et al., 2018).

Several other climate factors are also argued to influence the interannual variation of WNP TC activity (e.g., Huo et al., 2015; Zhan et al., 2013). For instance, it has been hypothesized that tropical North Atlantic SST anomalies are connected with the WNP TC genesis frequency via adjustments of the Walker Circulation (Huo et al., 2015; Yu et al., 2016; Zhang et al., 2017a). Furthermore, several studies hypothesized possible linkages between the Pacific Meridional Mode (PMM) and WNP TC activity (Gao et al., 2018; Hong et al., 2018; Wu et al., 2018; Zhan et al., 2017; Zhang et al., 2016; Zhang et al., 2017b). The PMM is the leading singular vector decomposition (SVD) mode of SST and 10-m wind vector over the central to eastern Pacific (21°S–32°N, 175°E–95°W) after linearly removing the

SST variability in the Pacific cold tongue (6°S–6°N, 90°W–150°W; Chiang & Vimont, 2004). This mode features a meridional seesaw of SST anomalies accompanied by cross-equatorial surface winds. It was previously argued that the PMM may serve as an ENSO-independent factor in statistical/hybrid models to improve seasonal forecasts of TC genesis frequency (Zhang et al., 2016, 2017b). It has also been found that the statistical PMM–WNP TC relationship is dominated by TC variability occurring in the southeastern part of the WNP (SE–WNP; Zhang et al., 2016). A statistical relationship between PMM and the number of intense TCs was also found (Gao et al., 2018) since intense TCs usually occur in the SE–WNP (Camargo & Sobel, 2005).

However, intriguingly the PMM exhibits no statistically significant correlation with the WNP large-scale circulation when examining a 19-year running correlation (see figure 5a of Hong et al., 2018), which seems to be inconsistent with these previous studies. So far, it is still unknown whether there exists an underlying dynamical basis for the statistical PMM–TC relationship and what the key processes are that might be bridging them. Further investigation is needed to deepen our understanding of WNP TC variability, which could potentially provide guidance for seasonal TC activity forecasts. Here, we demonstrate that the statistical relationship between PMM and SE–WNP TC genesis number is dominated by their co-variability on decadal timescales. Importantly, decadal PMM variability exhibits very similar temporal and spatial characteristics as CP ENSO-like SST variability on the quasi-decadal timescales. We also find that both the interannual and decadal components of the SE–WNP TC genesis frequency are correlated with the commonly used Niño3.4 index that describes ENSO variability.

2. Data and Methodology

Several atmospheric and oceanic reanalysis data sets are utilized including monthly horizontal wind from the NCEP–NCAR reanalysis (Kalnay et al., 1996) and SST from the National Oceanic and Atmospheric Administration (NOAA) Extended Reconstructed Sea Surface Temperature data set, version 5 (Huang et al., 2017). The best-track data sets for the WNP TC are derived from the Joint Typhoon Warning Center (JTWC), the Shanghai Typhoon Institute of the China Meteorology Administration (CMA), and the Regional Specialized Meteorological Center (RSMC) Tokyo–Typhoon Center, Japan Meteorological Agency (JMA). A TC is defined as such when the maximum sustained wind (MSW) speed reaches the critical value of 34 knots/s (17.5 m/s) for the JTWC and CMA data sets. For the JMA data, a TC is identified according to its category reaching at least the tropical storm intensity, due to unavailable MSW records before 1977. The PMM is characterized by the SVD-derived SST expansion coefficient index, which is provided by the University of Wisconsin–Madison. The CP El Niño index (CPI) was calculated based on the method outlined in Ren and Jin (2011).

Throughout the manuscript we focus on the TC active season (July–November). However, the conclusions remain unchanged if we use other TC season definitions such as June–November (not shown). Anomalies were calculated as the departures from the climatological monthly mean for the entire study period (1951–2017) and were linearly de-trended to remove possible influences of the long-term trend. To separate interannual and decadal variability, a 9-point Lanczos low-pass (low frequency [LF], i.e., decadal variability) and high-pass filter (high frequency [HF], i.e., interannual variability) with an 8-year cutoff period was applied to all climate indices and variables. Statistical significance for correlations and regressions were determined based on the two-tailed Student's *t* test. For the low-pass filtered variables, we calculated the effective sample size using the following equation (Bretherton et al., 1999):

$$N = N_{\text{eff}} \frac{1 - R_1 \times R_2}{1 + R_1 \times R_2},$$

where N , N_{eff} , R_1 , and R_2 represent sample size, effective sample size, and the auto-correlation of two samples at lag time one, respectively. We also use cross-spectral analysis to investigate the relationship between two signals. Ten percent of both time series were tapered with a split-cosine-bell taper before performing the Fast Fourier transform. With our choice of tapers the resulting degrees of freedom is 5. The confidence level for the magnitude-squared coherence is defined following Julian (1975).

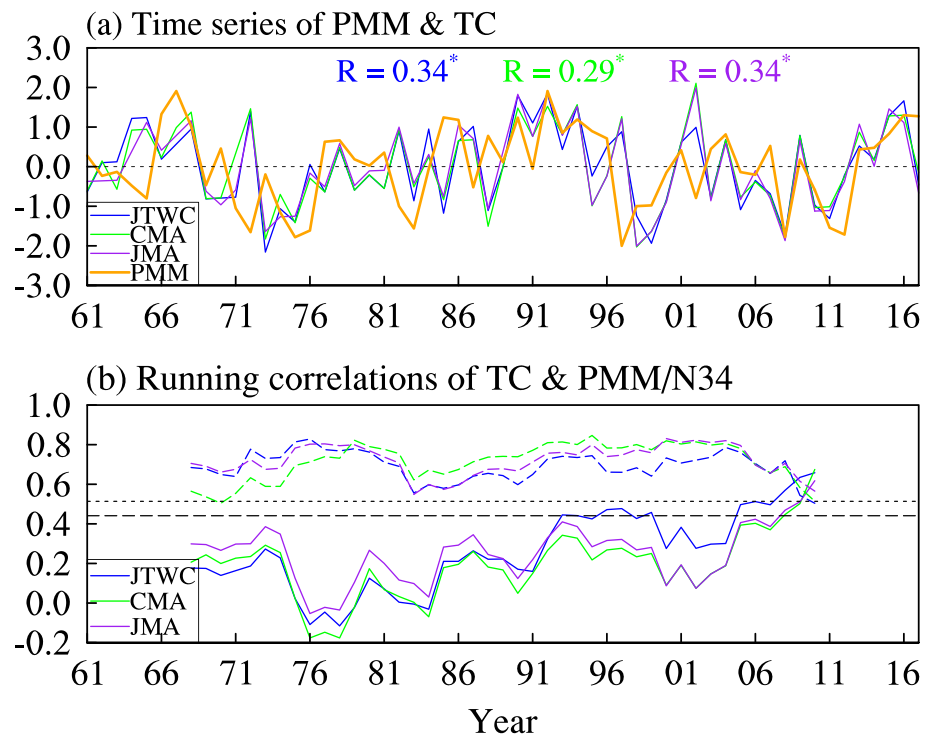


Figure 1. (a) Time evolutions of the normalized PMM index (averaged from July to November) and seasonal TC genesis number in the SE-WNP. (b) 15-year running correlations between the SE-WNP TC genesis number with the PMM (solid lines), as well as with Niño3.4 (dashed lines) indices. Blue, green, and purple lines indicate different TC data sources from the JTWC, CMA, and JMA, respectively. Correlation coefficients between the PMM and TC genesis number are shown in (a) with asterisk * indicating values that are statistically significant at the 95% confidence level. Two horizontal dashed lines in (b) denote the 90% and 95% confidence levels based on the two-tailed Student's *t* test.

We also use an atmospheric general circulation model (AGCM) developed by Geophysical Fluid Dynamics Laboratory (GFDL AM2.1; Anderson et al., 2004) to further confirm the atmospheric responses to SST patterns associated with the PMM on different timescales. We conducted three experiments: one control and two perturbation experiments. In the control (CTRL) simulation, we prescribe global monthly climatological SST and sea-ice concentration boundary conditions for the study period (i.e., 1951–2017). The two perturbation simulations are prepared by adding SST anomalies during the WNP TC season (i.e., July to November) obtained by regressing the normalized PMM-LF and PMM-HF indices onto the SST anomalies for the tropical Pacific region (30°S–30°N, 150°E–80°W; supporting information Figure S4). Each simulation consists of 25 ensemble members with different perturbed initial conditions.

3. Results

Figure 1 displays the relationship between the PMM index and TC genesis frequency over the southeastern subdomain of the WNP (0°–20°N, 140°E–180°). The seasonal (July–November) averaged TC genesis number from all three TC data sources (i.e., JTWC, CMA, and JMA) exhibits similar moderate correlations with the PMM index ($R \sim 0.3$; Figure 1a), consistent with previous finding (Zhang et al., 2016). We also conduct a 15-year running correlation (Figure 1b) to examine the long-term stability of their relationship. The PMM does not show any significant correlation with the TC number for almost the whole study period, except for recent years (the result is not sensitive to the choice of running window length). This indicates that the PMM does not modulate the interannual variability of the SE-WNP TC genesis frequency. As shown in previous studies, both the PMM (Stuecker, 2018) and TC genesis number (Liu et al., 2019) exhibit variability on multiple timescales, which is dominated by and can be separated into decadal and interannual components (Figure S1). Considering their insignificant interannual correlation, we expect that the observed moderate PMM-TC correlation is mainly caused by their co-variability at lower frequencies.

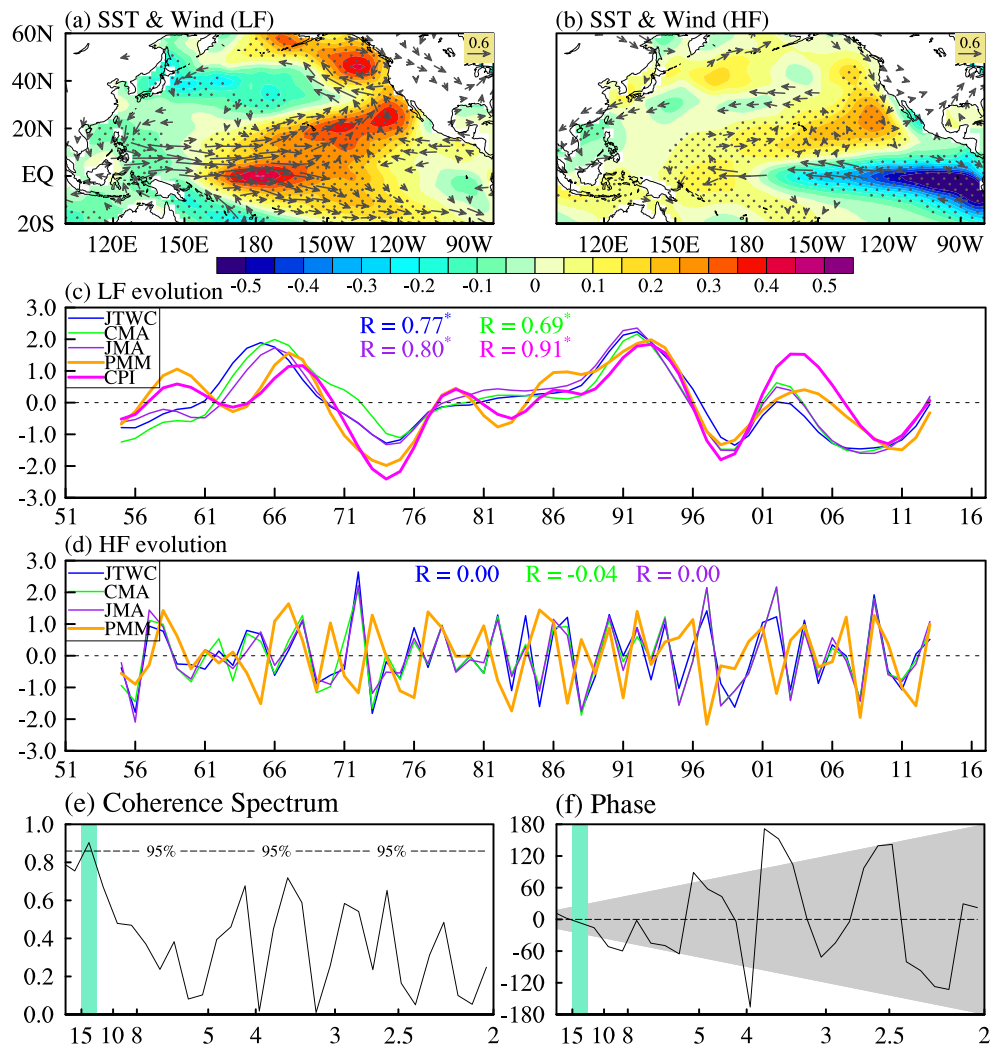


Figure 2. SST ($^{\circ}\text{C}$) and 850-hPa wind (m/s) anomalies regressed onto the normalized (a) low-frequency and (b) high-frequency components of the PMM index. (c) Time evolution of the low-frequency components of the PMM, CPI, and SE-WNP TC genesis number. (d) Time evolution of the high-frequency components of the PMM and SE-WNP TC genesis number. (e) Coherence spectrum and (f) corresponding phase (degree) relationship between the PMM and SE-WNP TC genesis number. In (a) and (b), only the values exceeding the 95% confidence level are stippled (SST) or shown (winds). In (c) and (d), the blue, green, and purple lines indicate TC data from JTWC, CMA, and JMA, respectively. Correlation coefficients between the PMM and different indices are shown in each plot with asterisk * indicating values that are statistically significant at the 95% confidence level. The horizontal dashed line in (e) denotes the 95% confidence level. In (f), positive phase angles mean that the PMM leads the TC genesis number. Green shading highlights the statistically significant periodicities at the 95% confidence level. Grey shading indicates phase angles that cannot be resolved given that yearly data are used.

We next investigate the influences of the PMM on SE-WNP TC genesis frequency on interannual and decadal timescales separately utilizing a 9-point Lanczos filter (Figure 2). Hereafter, the high- and low-frequency components of the PMM are denoted by PMM-HF and PMM-LF, respectively. Interestingly, the PMM-associated SST and low-level wind anomaly patterns are distinct on different timescales (Figures 2a and 2b). The SST anomaly pattern of the PMM-LF resembles the CP ENSO-like pattern (Figure S2), which is also evidenced by a high temporal correlation ($R = 0.91$) between the PMM-LF and CPI-LF (Figure 2c). In response to positive SST anomalies in the tropical central Pacific, we see anomalous low-level westerly winds over the western Pacific (Gill, 1980), which can affect the TC genesis frequency through its effect on vertical wind shear and vorticity. As expected, we see decreased zonal vertical wind shear and enhanced low-level vorticity over the SE-WNP during the positive PMM-LF phase, both of which are favorable conditions for

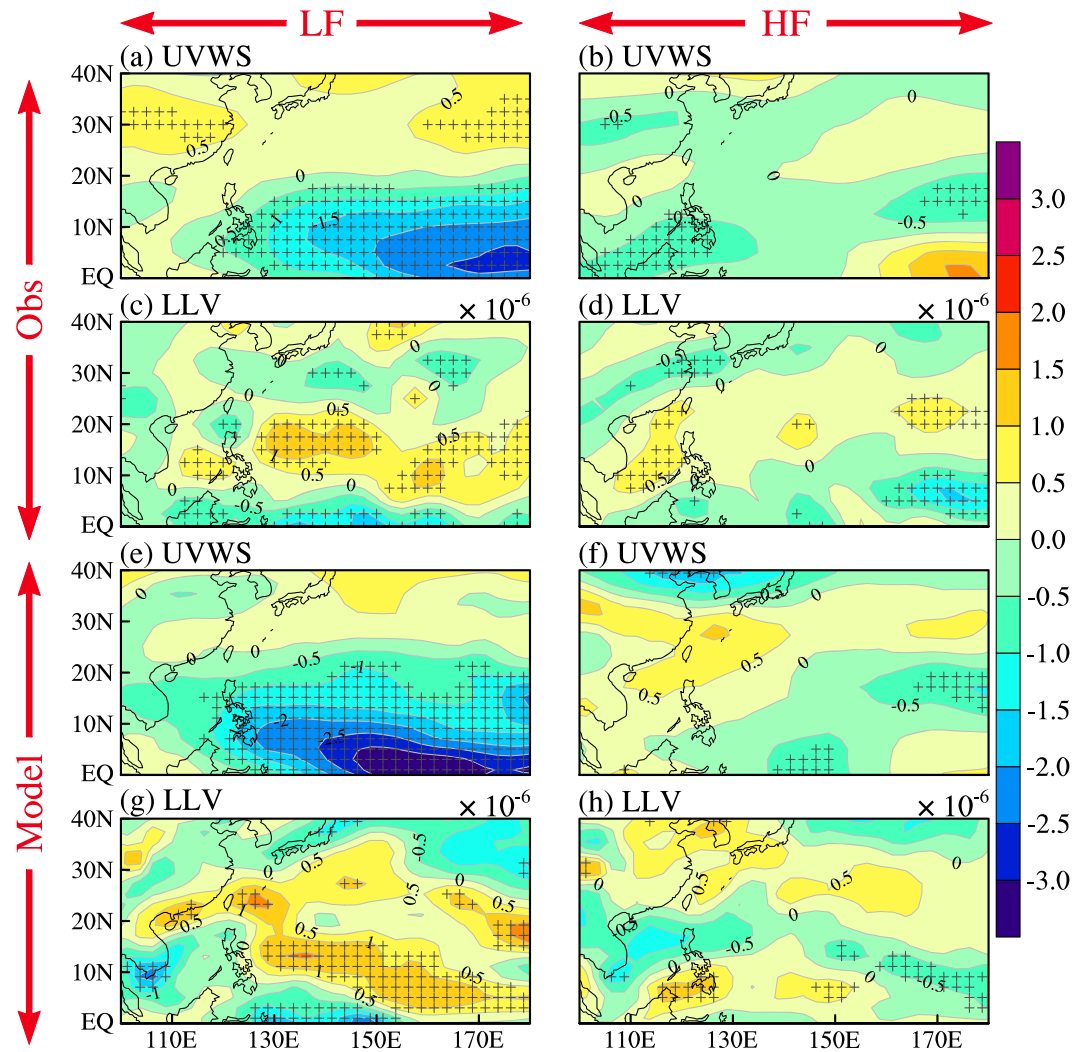


Figure 3. Observed (a) zonal vertical wind shear (m/s) between 200 and 850 hPa and (c) the relative vorticity (s^{-1}) at 850 hPa regressed onto the normalized low-frequency component of the PMM index. (b) and (d) are same as (a) and (c) but for the high-frequency component of the PMM index. Composite difference of (e) zonal vertical wind shear (m/s) between 200 and 850 hPa and (g) the relative vorticity (s^{-1}) at 850 hPa between PMM-LF and CTRL simulations. (f) and (h) are same as (e) and (g) but for the difference between PMM-HF and CTRL simulations. Values exceeding the 95% confidence level are stippled.

TC genesis (Figures 3a and 3c). Their relationship can also be supported by highly consistent time evolutions of the PMM and SE-WNP TC genesis number on decadal timescales ($R \sim 0.75$; Figure 2c). There are also SST anomalies present near the northeastern subtropical Pacific, which seem to be associated with the southwesterly wind anomalies through the positive Wind-Evaporation-SST (WES) feedback (e.g., Xie & Philander, 1994).

On interannual timescales, the PMM-associated SST pattern is characterized by a meridional dipole over the eastern Pacific (Figure 2b), which is similar to the unfiltered PMM pattern, but with slightly reduced magnitude in the subtropical northeast Pacific and increased magnitude over the equatorial eastern Pacific. Due to the relatively cold SST climatology in the equatorial cold tongue and subtropical northeastern Pacific, PMM-related atmospheric heating is weak in these regions (Figure S3a) considering the SST threshold for deep convection. Therefore, the related low-level circulation anomalies are also weak, including easterly wind anomalies in the equatorial eastern Pacific and an anomalously weak low-level cyclonic circulation near the Hawai'i islands (Figure 2b). Almost no statistically significant large-scale circulation anomalies can be detected over the SE-WNP. Accordingly, the anomalies of the zonal vertical wind shear

and enhanced low-level vorticity are small over the WNP except for a few local regions (Figures 3b and 3d). Thus, we conclude that the PMM-HF has no pronounced impact on TC variability over the SE-WNP, which is also supported by the fact that these indices show no temporal correlation ($R \sim 0$; Figure 2d).

The above analyses show that the climate variability described by the PMM index has remarkably distinct impacts on SE-WNP TC variability depending on the timescale. Next, we apply a cross-spectral analysis between the indices to reveal potential coherence and phase differences as a function of periodicity (Figures 2e and 2f). The PMM and SE-WNP TC frequency show significant coherence only on low-frequency quasi-decadal timescales (~ 12 years periodicity), which further supports our conclusions. The distinct atmospheric circulation responses to PMM-LF and PMM-HF SST anomaly patterns that affect TC genesis numbers are also validated in AGCM experiments (Figures 3e–3h). Our results suggest that the PMM cannot serve as a potential factor for improving the seasonal forecast of WNP TC activities. In addition, when investigating the standard PMM index that includes variability on all timescales, the PMM-HF component seems to obscure the robust relationship between the PMM-LF and UVWS, thus resulting in the observed weak relationship between the PMM and UVWS in the SE-WNP (Larson et al., 2012).

We next focus on the role of tropical SST variability, as the PMM-LF exhibits similar spatial and temporal characteristics as CP ENSO-like quasi-decadal variability (Stuecker, 2018). Previous studies have also demonstrated that tropical SST variability has a strong modulating effect on year-to-year SE-WNP TC variations (e.g., Chen & Tam, 2010; Wang & Chan, 2002). Therefore, it is natural to investigate whether we can capture decadal TC variability with a unified tropical Pacific SST anomaly index. We find that indeed the commonly used Niño3.4 index is correlated on both decadal and interannual timescales with the SE-WNP TC genesis number. The Niño3.4 region covers the central-to-eastern tropical Pacific and exhibits pronounced SST variability both on interannual and quasi-decadal timescales (Figure 4).

The SST and low-level wind anomalies associated with the decadal Niño3.4 component are almost the same as those associated with the PMM-LF (Figure 2a) and CPI decadal component (Figure S2a) with only small differences in the far eastern tropical Pacific. On interannual timescales, the typical ENSO features are described by the Niño3.4 index (Figure 4b), which has been demonstrated to be an important forcing for the year-to-year variations of the SE-WNP TC number (Wang & Chan, 2002). During El Niño events, the anomalous SST warming over the equatorial central Pacific gives rise to strong atmospheric convection (Figure S3b), which can alter the zonal vertical wind shear and low-level vorticity over the SE-WNP in a Gill-type response and thereby affect the local TC genesis number. This is indicated by a significant correlation ($R \sim 0.65$) between Niño3.4 and SE-WNP TC number on interannual timescales (Figure 4d). This year-to-year relationship exhibits a high long-term stability over the entire time period, very different from the PMM relationship with the SW-WNP TC number (Figure 1b). Furthermore, on decadal timescales we also observe a high correlation ($R \sim 0.75$) between the Niño3.4 index and the SE-WNP TC number (Figure 4c). The cross-spectral analysis further confirms simultaneous co-variability between tropical Pacific SST anomalies (i.e., Niño3.4 index) and SE-WNP TC genesis number both on interannual and decadal timescales. The above results suggest that both interannual and decadal variability of the SE-WNP TC genesis number are related to central tropical Pacific SST variability and not to off-equatorial SST patterns.

4. Discussion

Our analyses demonstrate that a statistically significant relationship between the PMM and SE-WNP TC genesis number only exists on decadal timescales (and not on interannual timescales). The low-frequency component of the PMM resembles the CP ENSO-like SST pattern, which can modulate the zonal vertical wind shear and low-level vorticity and thus the TC genesis number over the SE-WNP. We further demonstrate that both interannual and quasi-decadal variability of the SE-WNP TC number are closely related to tropical SST variability described by the Niño3.4 index. Thus, equatorial Pacific SST variability could provide a potential source for SE-WNP TC predictability on both interannual and decadal timescales.

We also examine possible relationships of the PMM with other climate indices to understand their potential physical linkages (Figure S5). Compared to the high correlation between the PMM-LF and CPI ($R = 0.91$) on decadal timescales, we find no statistically significant correlation between PMM-LF and the Pacific Decadal Oscillation (PDO) index ($R = 0.47$), although they are co-varying roughly in-phase since the early 1990s. A review paper (Newman et al., 2016) documented that the PDO can be generalized as a red noise process that

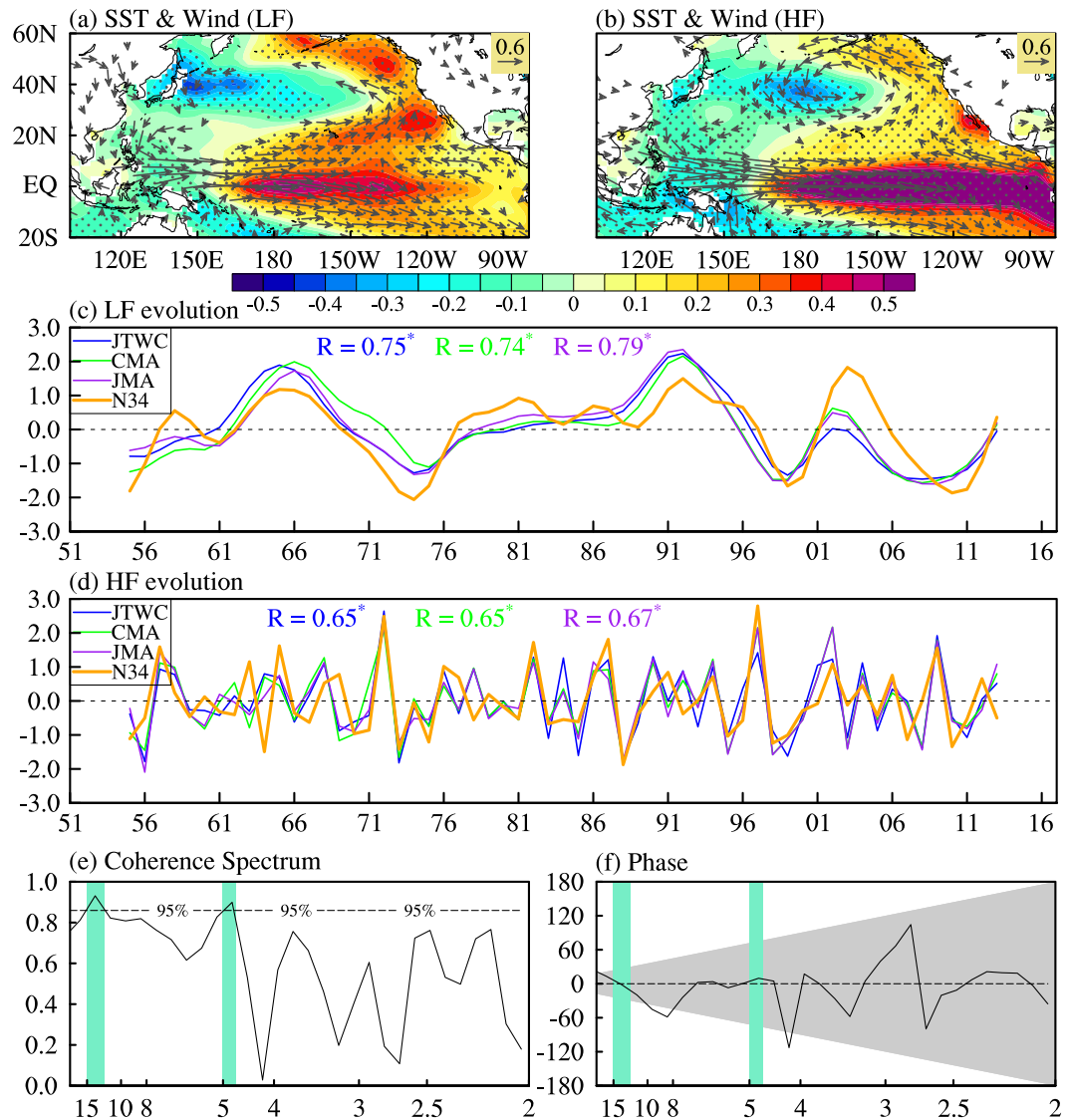


Figure 4. SST ($^{\circ}\text{C}$) and 850-hPa wind (m/s) anomalies regressed onto the normalized (a) low-frequency and (b) high-frequency components of the Niño3.4 index. (c) Time evolution of the low-frequency components of the Niño3.4, and SE-WNP TC genesis number. (d) Time evolution of the high-frequency components of the Niño3.4 and SE-WNP TC genesis number. (e) Coherence spectrum and (f) corresponding phase (degree) relationship between the Niño3.4 and SE-WNP TC genesis number. In (a) and (b), only the values exceeding the 95% confidence level are stippled (SST) or shown (winds). In (c) and (d), the blue, green, and purple lines indicate TC data from JTWC, CMA, and JMA, respectively. Correlation coefficients between the Niño3.4 and different indices are shown in each plot with asterisk * indicating values that are statistically significant at the 95% confidence level. The horizontal dashed line in (e) denotes the 95% confidence level. In (f), positive phase angles mean that the Niño3.4 leads the TC genesis number. Green shading highlights the statistically significant periodicities at the 95% confidence level. Grey shading indicates phase angles that cannot be resolved given that yearly data are used.

integrates both local North Pacific atmospheric noise forcing and remote forcing from tropical Pacific SST. Therefore, we hypothesize that part of the increased correlation between PDO and PMM-LF in recent decades might be explained by strengthened quasi-decadal tropical Pacific SST variability (Figure S6). The North Pacific Gyre Oscillation (NPGO) index closely follows the decadal swings of both PMM-LF and CPI with about 1-year lag ($R = 0.73$; the sign of NPGO reversed), consistent with previous results that SST variability over the tropical central Pacific can partly drive NPGO variability (Di Lorenzo et al., 2010; Stuecker, 2018). Moreover, it seems that the PMM-LF component describes the same physical process as

central Pacific quasi-decadal SST variability and is somewhat different from extra-tropical SST variability (e.g., the PDO). On interannual timescales, the variability of the PMM-HF is partly explained by SST variability over Niño1+2 region ($R = 0.62$, statistically significant at the 95% confidence level), suggesting that coastal air-sea coupled processes could be associated with interannual variations of the PMM.

Previous studies documented a prominent decadal decrease of the WNP TC genesis number around the mid-to-late of 1990s, which was mainly attributed to the TC genesis decrease in the SE-WNP (e.g., Hong et al., 2016; Liu et al., 2019; Liu & Chan, 2013). Several modulating processes were proposed to understand this decadal change, such as phase transitions of either the Atlantic Multidecadal Oscillation (AMO) or the PDO (e.g., Hong et al., 2016; Liu & Chan, 2013; Zhang et al., 2018). The AMO and PDO indices mainly represent multidecadal variability outside the tropical Pacific (e.g., Mantua et al., 1997; Trenberth & Shea, 2006), which are distinct from the central tropical Pacific quasi-decadal variability investigated in this study. Their modulation effect on the SE-WNP TC decadal variability seems to be only a minor factor in observations (Liu et al., 2019). In contrast, the importance of central tropical Pacific SST variability on decadal variations of WNP TC frequency has been noted by a few modeling studies (Matsuura et al., 2003; Mei et al., 2015).

One recent study found that the raw PMM index shows nearly identical co-variability with the CPI on both interannual and decadal timescales (Stuecker, 2018). We emphasize that the raw PMM index used in Stuecker (2018) is not the same as the filtered PMM index used in our study (see <http://www.aos.wisc.edu/~dvmont/MModes/PMM.html> for more details on their definitions). The decadal components of both the PMM and raw PMM show similar spatial patterns as the CP ENSO-like pattern and exhibit consistent relationships with the SE-WNP TC (Figures 2a, 3a and 3c, S7a, S7c, and S7e). In contrast, while on interannual timescales the raw PMM also features the CP ENSO-like pattern, the PMM shows a pronounced meridional SST dipole in the eastern Pacific. This suggests that the PMM indices, especially on interannual timescales, are highly sensitive to processing methods and definitions. Hence, we emphasize that caution is required when interpreting the statistical relationship between the PMM and other climate factors on interannual timescales.

Acknowledgments

Reanalysis data sets used in this paper are available from <https://www.esrl.noaa.gov/psd/data/gridded/data.ncep.reanalysis.pressure.html> and <https://www.esrl.noaa.gov/psd/data/gridded/data.noaa.ersst.v5.html>. The tropical cyclone best-track data sets are located at <https://www.metoc.navy.mil/jtwc/jtwc.html?western-pacific> (JTWc), http://tcdata.typhoon.org.cn/zjljsj_zlqh.html (CMA), and <http://www.jma.go.jp/jma/jma-eng/jma-center/rsmc-hp-pub-eg/besttrack.html> (JMA). The PMM index is provided by the University of Wisconsin-Madison (<http://www.aos.wisc.edu/~dvmont/MModes/RealTime/PMM.txt>). This work was supported by the National Nature Science Foundation of China (41675073), the SOA Program on Global Change and Air-Sea interactions (GASI-IPOVAI-03), and the National Key Research and Development Program (2018YFC1506002). F.-F. Jin was supported by the U.S. National Science Foundation Grant AGS-1406601, and the U.S. Department of Energy Grant DE-SC000511. M. F. Stuecker was supported by the Institute for Basic Science (Project code IBS-R028-D1).

References

- Anderson, J. L., Balaji, V., Broccoli, A. J., Cooke, W. F., Delworth, T. L., Dixon, K. W., et al. (2004). The new GFDL global atmosphere and land model AM2-LM2: Evaluation with prescribed SST simulations. *Journal of Climate*, 17(24), 4641–4673. <https://doi.org/10.1175/JCLI-3223.1>
- Ashok, K., Behera, S. K., Rao, S. A., Weng, H. Y., & Yamagata, T. (2007). El Niño Modoki and its possible teleconnection. *Journal of Geophysical Research*, 112, C11007. <https://doi.org/10.1029/2006JC003798>
- Bretherton, C. S., Widmann, M., Dymnikov, V. P., Wallace, J. M., & Blade, I. (1999). The effective number of spatial degrees of freedom of a time-varying field. *Journal of Climate*, 12, 20.
- Camargo, S. J., Emanuel, K. A., & Sobel, A. H. (2007). Use of a genesis potential index to diagnose ENSO effects on tropical cyclone genesis. *Journal of Climate*, 20(19), 4819–4834. <https://doi.org/10.1175/JCLI4282.1>
- Camargo, S. J., & Sobel, A. H. (2005). Western North Pacific tropical cyclone intensity and ENSO. *Journal of Climate*, 18(15), 2996–3006. <https://doi.org/10.1175/JCLI3457.1>
- Chen, G., & Tam, C.-Y. (2010). Different impacts of two kinds of Pacific Ocean warming on tropical cyclone frequency over the western North Pacific. *Geophysical Research Letters*, 37(1), L01803. <https://doi.org/10.1029/2009GL041708>
- Chiang, J. C. H., & Vimont, D. J. (2004). Analogous Pacific and Atlantic meridional modes of tropical atmosphere–ocean variability. *Journal of Climate*, 17, 16.
- Di Lorenzo, E., Cobb, K. M., Furtado, J. C., Schneider, N., Anderson, B. T., Bracco, A., et al. (2010). Central Pacific El Niño and decadal climate change in the North Pacific Ocean. *Nature Geoscience*, 3(11), 762–765. <https://doi.org/10.1038/ngeo984>
- Du, Y., Yang, L., & Xie, S.-P. (2011). Tropical Indian Ocean influence on northwest Pacific tropical cyclones in summer following strong El Niño. *Journal of Climate*, 24(1), 315–322. <https://doi.org/10.1175/2010JCLI3890.1>
- Gao, S., Zhu, L., Zhang, W., & Chen, Z. (2018). Strong modulation of the Pacific meridional mode on the occurrence of intense tropical cyclones over the western North Pacific. *Journal of Climate*, 31(19), 7739–7749. <https://doi.org/10.1175/JCLI-D-17-0833.1>
- Gill, A. E. (1980). Some simple solutions for heat-induced tropical circulation. *Quarterly Journal of the Royal Meteorological Society*, 106(449), 447–462. <https://doi.org/10.1002/qj.49710644905>
- Hong, C.-C., Lee, M.-Y., Hsu, H.-H., & Tseng, W.-L. (2018). Distinct influences of the ENSO-like and PMM-like SST anomalies on the mean TC genesis location in the western North Pacific: The 2015 summer as an extreme example. *Journal of Climate*, 31(8), 3049–3059. <https://doi.org/10.1175/JCLI-D-17-0504.1>
- Hong, C.-C., Wu, Y.-K., & Li, T. (2016). Influence of climate regime shift on the interdecadal change in tropical cyclone activity over the Pacific Basin during the middle to late 1990s. *Climate Dynamics*, 47(7–8), 2587–2600. <https://doi.org/10.1007/s00382-016-2986-x>
- Huang, B., Thorne, M. P., Banzon, F. V., Boyer, T., Chepurin, G., Lawrimore, J. H., et al. (2017). Extended Reconstructed Sea Surface Temperature, Version 5 (ERSSTv5): Upgrades, validations, and intercomparisons. *Journal of Climate*, 30(20), 8179–8205. <https://doi.org/10.1175/JCLI-D-16-0836.1>
- Huo, L., Guo, P., Hameed, S. N., & Jin, D. (2015). The role of tropical Atlantic SST anomalies in modulating western North Pacific tropical cyclone genesis. *Geophysical Research Letters*, 42, 2378–2384. <https://doi.org/10.1002/2015GL063184>

- Julian, P. R. (1975). Comments on the determination of significance levels of the coherence statistics. *Journal of the Atmospheric Sciences*, 32, 836–837.
- Kalnay, E., Kanamitsu, M., Kistler, R., Collins, W., Deaven, D., Gandin, L., et al. (1996). The NCEP/NCAR 40-year reanalysis project. *Bulletin of the American Meteorological Society*, 77(3), 437–471. [https://doi.org/10.1175/1520-0477\(1996\)077<0437:TNYRP>2.0.CO;2](https://doi.org/10.1175/1520-0477(1996)077<0437:TNYRP>2.0.CO;2)
- Kao, H.-Y., & Yu, J.-Y. (2009). Contrasting eastern-Pacific and central-Pacific types of ENSO. *Journal of Climate*, 22(3), 615–632. <https://doi.org/10.1175/2008JCLI2309.1>
- Kim, H.-M., Webster, P. J., & Curry, J. A. (2011). Modulation of North Pacific tropical cyclone activity by three phases of ENSO. *Journal of Climate*, 24(6), 1839–1849. <https://doi.org/10.1175/2010JCLI3939.1>
- Kug, J.-S., Jin, F.-F., & An, S.-I. (2009). Two types of El Niño events: Cold tongue El Niño and warm pool El Niño. *Journal of Climate*, 22(6), 1499–1515. <https://doi.org/10.1175/2008JCLI2624.1>
- Larson, S., Lee, S.-K., Wang, C., Chung, E.-S., & Enfield, D. (2012). Impacts of non-canonical El Niño patterns on Atlantic hurricane activity: Non-canonical El Niños and hurricanes. *Geophysical Research Letters*, 39(14), L14706. <https://doi.org/10.1029/2012GL052595>
- Liu, C., Zhang, W., Geng, X., Stuecker, M. F., & Jin, F.-F. (2019). Modulation of tropical cyclones in the southeastern part of western North Pacific by tropical Pacific decadal variability. *Climate Dynamics*, 53(7-8), 4475–4488. <https://doi.org/10.1007/s00382-019-04799-w>
- Liu, K. S., & Chan, J. C. L. (2013). Inactive period of western North Pacific tropical cyclone activity in 1998–2011. *Journal of Climate*, 26(8), 2614–2630. <https://doi.org/10.1175/JCLI-D-12-00053.1>
- Mantua, N. J., Hare, S. R., Zhang, Y., Wallace, J. M., & Francis, R. C. (1997). A Pacific Interdecadal Climate Oscillation with impacts on salmon production. *Bulletin of the American Meteorological Society*, 78(6), 1069–1079. [https://doi.org/10.1175/1520-0477\(1997\)078<1069:APICOW>2.0.CO;2](https://doi.org/10.1175/1520-0477(1997)078<1069:APICOW>2.0.CO;2)
- Matsuura, T., Yumoto, M., & Iizuka, S. (2003). A mechanism of interdecadal variability of tropical cyclone activity over the western North Pacific. *Climate Dynamics*, 21(2), 105–117. <https://doi.org/10.1007/s00382-003-0327-3>
- McPhaden, M. J., Zebiak, S. E., & Glantz, M. H. (2006). ENSO as an integrating concept in Earth Science. *Science*, 314(5806), 1740–1745. <https://doi.org/10.1126/science.1132588>
- Mei, W., Xie, S.-P., Zhao, M., & Wang, Y. (2015). Forced and internal variability of tropical cyclone track density in the western North Pacific*. *Journal of Climate*, 28(1), 143–167. <https://doi.org/10.1175/JCLI-D-14-00164.1>
- Newman, M., Alexander, M. A., Ault, T. R., Cobb, K. M., Deser, C., Di Lorenzo, E., et al. (2016). The Pacific Decadal Oscillation, revisited. *Journal of Climate*, 29(12), 4399–4427. <https://doi.org/10.1175/JCLI-D-15-0508.1>
- Ren, H.-L., & Jin, F.-F. (2011). Niño indices for two types of ENSO. *Geophysical Research Letters*, 38(4), L04704. <https://doi.org/10.1029/2010GL046031>
- Stuecker, M. F. (2018). Revisiting the Pacific Meridional Mode. *Scientific Reports*, 8(1). <https://doi.org/10.1038/s41598-018-21537-0>
- Timmermann, A., An, S.-I., Kug, J.-S., Jin, F.-F., Cai, W., Capotondi, A., et al. (2018). El Niño–Southern Oscillation complexity. *Nature*, 559(7715), 535–545. <https://doi.org/10.1038/s41586-018-0252-6>
- Trenberth, K. E., & Shea, D. J. (2006). Atlantic hurricanes and natural variability in 2005. *Geophysical Research Letters*, 33, L12704. <https://doi.org/10.1029/2006GL026894>
- Wallace, J. M., Rasmusson, E. M., Mitchell, T. P., Kousky, V. E., Sarachik, E. S., & von Storch, H. (1998). On the structure and evolution of ENSO-related climate variability in the tropical Pacific: Lessons from TOGA. *Journal of Geophysical Research - Oceans*, 103(C7), 14241–14259. <https://doi.org/10.1029/97JC02905>
- Wang, B., & Chan, J. C. (2002). How strong ENSO events affect tropical storm activity over the western North Pacific. *Journal of Climate*, 15(13), 1643–1658.
- Wang, C., Li, C., Mu, M., & Duan, W. (2013). Seasonal modulations of different impacts of two types of ENSO events on tropical cyclone activity in the western North Pacific. *Climate Dynamics*, 40(11–12), 2887–2902. <https://doi.org/10.1007/s00382-012-1434-9>
- Wang, C., Wang, B., & Wu, L. (2018). Abrupt breakdown of the predictability of early season typhoon frequency at the beginning of the twenty-first century. *Climate Dynamics*, 52(7-8), 3809–3822. <https://doi.org/10.1007/s00382-018-4350-9>
- Wu, Y.-K., Hong, C.-C., & Chen, C.-T. (2018). Distinct effects of the two strong El Niño events in 2015–2016 and 1997–1998 on the western North Pacific Monsoon and tropical cyclone activity: Role of subtropical eastern North Pacific warm SSTA. *Journal of Geophysical Research: Oceans*, 123(5), 3603–3618. <https://doi.org/10.1002/2018JC013798>
- Xie, S.-P., & Philander, S. G. H. (1994). A coupled ocean-atmosphere model of relevance to the ITCZ in the eastern Pacific. *Tellus*, 46A, 340–350.
- Yu, J., Li, T., Tan, Z., & Zhu, Z. (2016). Effects of tropical North Atlantic SST on tropical cyclone genesis in the western North Pacific. *Climate Dynamics*, 46(3–4), 865–877. <https://doi.org/10.1007/s00382-015-2618-x>
- Zhan, R., Wang, Y., & Liu, Q. (2017). Salient differences in tropical cyclone activity over the western North Pacific between 1998 and 2016. *Journal of Climate*, 30(24), 9979–9997. <https://doi.org/10.1175/JCLI-D-17-0263.1>
- Zhan, R., Wang, Y., & Wen, M. (2013). The SST gradient between the southwestern Pacific and the western Pacific warm pool: A new factor controlling the northwestern Pacific tropical cyclone genesis frequency. *Journal of Climate*, 26(7), 2408–2415. <https://doi.org/10.1175/JCLI-D-12-00798.1>
- Zhang, W., Vecchi, G. A., Murakami, H., Villarini, G., Delworth, T. L., Yang, X., & Jia, L. (2018). Dominant role of Atlantic Multidecadal Oscillation in the recent decadal changes in western North Pacific tropical cyclone activity. *Geophysical Research Letters*, 45(1), 354–362. <https://doi.org/10.1002/2017GL076397>
- Zhang, W., Vecchi, G. A., Murakami, H., Villarini, G., & Jia, L. (2016). The Pacific Meridional Mode and the occurrence of tropical cyclones in the western North Pacific. *Journal of Climate*, 29(1), 381–398. <https://doi.org/10.1175/JCLI-D-15-0282.1>
- Zhang, W., Vecchi, G. A., Villarini, G., Murakami, H., Gudgel, R., & Yang, X. (2017b). Statistical–dynamical seasonal forecast of western North Pacific and East Asia landfalling tropical cyclones using the GFDL FLOR coupled climate model. *Journal of Climate*, 30(6), 2209–2232. <https://doi.org/10.1175/JCLI-D-16-0487.1>
- Zhang, W., Vecchi, G. A., Villarini, G., Murakami, H., Rosati, A., Yang, X., et al. (2017a). Modulation of western North Pacific tropical cyclone activity by the Atlantic Meridional Mode. *Climate Dynamics*, 48(1–2), 631–647. <https://doi.org/10.1007/s00382-016-3099-2>